Variation in the Spectral Content of UHF PD Signals Due to the Presence of Obstacles in the Measurement Environment

Jorge Alfredo Ardila-Rey, *Member, IEEE*, Bruno Albuquerque de Castro, *Senior Member, IEEE*, Rodrigo Rozas-Valderrama, Luis Orellana, Carlos Boya, Firdaus Muhammad-Sukki, and Abdullahi Abubakar Mas'ud

***Abstract*—Partial discharge (PD) detection is crucial to diagnose the condition of the insulation system of high-voltage equipment. Despite the existence of many different methods to monitor the presence of PD, ultrahigh frequency (UHF) methods are frequently used since galvanic contact between the antenna and the equipment under test is not required during the measurement. However, the measurement of electromagnetic (EM) emissions using antennas may be influenced not only by noise from outside sources but also by reflections or changes in the signals caused by obstacles in the measurement environment. This work presents the results of a series of experimental measurements that led to characterizing the spectral behavior of the PD signals captured with a Vivaldi antenna in the presence of two different configurations of obstacles located in the vicinity of the PD emission source. From these results, it was possible to establish that the spectral content of the PD signals in UHF changes for certain bands or frequency intervals depending on the shape of the obstacles located in the measurement environment. Likewise, it was evidenced that the changes in the signals can modify the characteristic parameters based on the spectral behavior of the signals, generating variations in the results obtained in the processes of separation and identification of sources.**

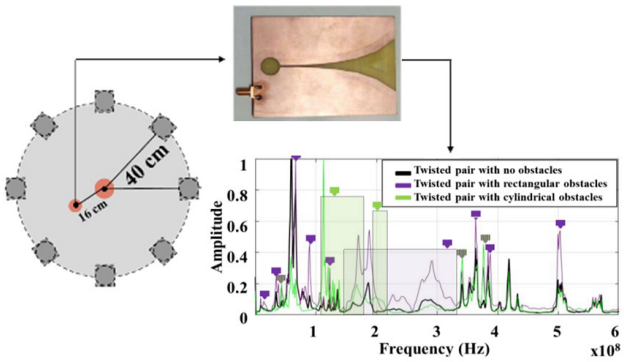

***Index Terms*— Fault diagnosis, partial discharges (PDs), ultrahigh frequency (UHF), Vivaldi antenna signal processing.**

The authors would like to express their appreciation to National Research and Development Agency (ANID) for the support received through the projects Fondecyt regular 1230135 and Fondef ID22I10153. The associate editor coordinating the review of this article and approv-ing it for publication was Dr. Rajan Jha. *(Corresponding author: Jorge Alfredo Ardila-Rey.)*

Jorge Alfredo Ardila-Rey and Rodrigo Rozas-Valderrama are with the Department of Electrical Engineering, Universidad Técnica Federico Santa María, Santiago 8940000, Chile (e-mail: jorge.ardila@usm.cl; rodrigo.
rozas@usm.cl).

Bruno Albuquerque de Castro is with the Department of Electrical Engineering, Sao Paulo State University, 17033-360 Sao Paulo, Brazil (e-mail: bruno.castro@unesp.br).

Luis Orellana is with the Karlsruhe Institute of Technology (KIT), Institute for Pulsed Power and Microwave Technology (IHM), 76344 Eggenstein-Leopoldshafen, Germany (e-mail: luis.orellana@kit.edu).

Carlos Boya is with the Escuela Tecnológica Industrial, Instituto Técnico Superior Especializado (ITSE), Panama City 07215, Panama (e-mail: cboya@itse.ac.pa).

Firdaus Muhammad-Sukki is with the School of Computing, Engineering and the Built Environment, Edinburgh Napier University, EH10 5DT Edinburgh, U.K. (e-mail: f.muhammadsukki@napier.ac.uk).

Abdullahi Abubakar Mas'ud is with the Department of Electrical Engineering, Jubail Industrial College, Jubail 31961, Saudi Arabia (e-mail: abdullahi.masud@gmail.com).

I. Introduction

EARLY identification of failure in the insulation system of equipment and electrical machines in power utilities can help to avoid large economic losses associated with the change of the asset, new equipment acquisition, interruption of service, fines, civil lawsuits, or the loss of credibility on the part of the users [1], [2]. Consequently, it is of great importance to have reliable monitoring systems that allow continuous supervision of electrical assets to carry on adequate maintenance based on the current condition of the equipment [1], [2], [3], [4], [5]. Partial discharge (PD) monitoring is one of the main tools when estimating the degradation of the insulation system of any electrical asset subjected to high voltage [1]. These discharges tend to occur in the weakest points of the material such as voids, electrical trees, surface conductive particles, or sharp metallic protrusions [4], causing progressive deterioration of the dielectric properties of the insulation until failure finally occurs and the asset is disconnected from the grid. According to the nature of the failure, PD activity can give rise to various macroscopic effects such as physical–chemical reactions, electromagnetic (EM) radiation (visible, ultraviolet, and ultrahigh frequency (UHF) signals), current pulses, dielectric loss leading to heat

generation, and acoustic noise [1] and [5]. These effects stem from the repetitive energy exchange, as numerous pulses can be generated within a network cycle. Given the impulsive behavior of this degradation phenomenon, PD generates high-bandwidth EM emissions, validating the use of UHF antennas as a measurement method.

These antennas can be strategically deployed in the vicinity of the emission source to identify new failures or monitor the progress of a previously identified problem without the need for galvanized contact with the assets [5], [6], [7], [8]. In this sense, different studies have validated the use of antennas in the processes of separation, identification, and location of PD sources, even when multiple sources are simultaneously acting on one equipment [8], [9], [10]. Some of these works have also focused on characterizing and mitigating the negative effects that occur in UHF detection systems due to factors external to the emission source. Specifically, one of the most studied phenomena is the influence of external sources of noise, such as frequency modulation (FM), digital television (TV), global system for mobile communications (GSM), and wireless fidelity (Wi-Fi), which are issued at different frequency bands and can hide the presence of PD signals [11], [12], [13], [14]. As a result of these works, different noise mitigation techniques have been established that have proven to be very effective in industrial environments, where it is common to find multiple noise sources [15], [16]. Reflection and refraction effects experienced by EM waves emitted by the PDs due to the physical changes in the measurement environment are also of great interest in monitoring PD in UHF [17], [18]. A large part of the variations experienced by these signals is associated with the removal or inclusion of surrounding obstacles close to the emission source such as metallic structures of electrical machines, poles, towers, and bus bars. Most of the works addressing this problem have focused mainly on the processes of locating PD sources, since, as has been shown, these variations in the signals reduce the effectiveness of the location techniques, as it is not possible to accurately establish the time difference of arrival (TDOA), causing important errors in the algorithms utilized, especially when applied in 3-D spaces. Thanks to the results obtained, different solutions to this problem have been established, such as including the dimensionality of the obstacles and the measurement environment in the location algorithms, which has made it possible to obtain relatively small errors in the location processes [19]. Although many of these developments have significantly helped improve location processes no study to date has focused on evaluating whether the reflection or refraction of PD UHF signals in measurement environments can significantly alter the processes of separation and identification of PD sources. As described later in Section II, many of the source separation or identification techniques are based on the temporal and spectral behavior of the captured signals and any change made in the measurement environment could generate changes in signals from any type of source. Since the characteristic parameters used in the separation and identification techniques can become very sensitive to signal variations [7], [8], [9], [10], [11], the false positives or false alarms could be generated regarding the real condition of the source being monitored. In this article, the variations in the spectral power content experienced by EM emissions for two different PD sources due to the presence of obstacles in the measurement environments are studied. According to the results described in Section IV, it was possible to establish, for a Vivaldi antenna, the bands or frequency intervals where the spectral content is altered because of the constructive and destructive interference of the waves that reflect or refract in each obstacle. Additionally, the principal component analysis (PCA) and the chromatic technique applied to the obtained signals confirmed a variation in the characteristic parameters of the signals due to the presence of obstacles in the measurement environment, thus generating significant alterations in the results provided by some of the source separation and identification techniques.

II. Separation and Identification of PD Sources

A phase-resolved PD (PRPD) pattern visualizes the magnitude and time of occurrence of the PD pulses taking the network voltage (50–60 Hz) as a Álvarez et al. [13], Zhang et al. [15], and Javandel et al. [20]. Since each type of PD source exhibits a characteristic PRPD pattern regardless of the type of insulation system where it is occurring, the identification of PD sources can be done through visual interpretation of these patterns [20]. For any specialist or intelligent PD identification system, one of the main problems when analyzing and interpreting a PRPD pattern is the simultaneous presence of multiple sources of PD or electrical noise, which is very common in industrial environments. The patterns obtained under these conditions are generally difficult to interpret because the sources of greater amplitude and more representative in a number of pulses tend to hide the presence of other types of sources that could be much more harmful but with less amplitude and/or occurrence [20], [21].

Based on the above, a large part of the methodologies developed for the identification of PD includes a previous separation process to differentiate and isolate each source of PD and noise captured during measurement processes, see Fig. 1. Many of the separation techniques implemented use characteristic parameters extracted from the signals themselves, taking as reference the temporal and/or spectral behavior of the signals [20], [21], [22], [23], [24]. Therefore, to obtain adequate results from any separation process or technique, the characteristic parameters being used must be sufficiently sensitive to the small temporal or spectral changes of the signals from the different sources [7], [8], [9], [10], [11], [14], [15], [16], [17]. In this way, it is possible to classify the sources of PD and/or electrical noise in clusters to be distributed in different zones of a 2-D or 3-D separation map (according to the number of characteristic parameters used). Once the separation of the sources has been established, the subsequent identification process will be carried out more easily through the individual analysis of the PRPD patterns associated with each cluster found [20]. An important number of source separation techniques implemented so far are based mainly on the spectral behavior of PD pulses. For the technique described in [25] and [26] one of the two characteristic parameters used to separate the PD sources

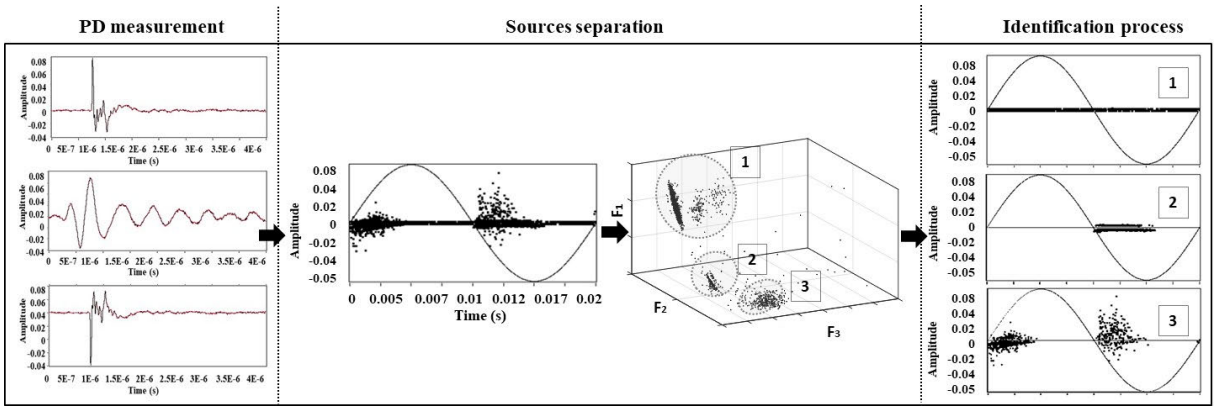

Fig. 1. Process of measurement, separation, and identification of PD sources.

2-D uses the standard deviation of the normalized signal in the frequency domain (F). In [27], [28], [29], and [30], the two characteristic parameters used in source separation are based on the spectral power ratio high (PRH) and spectral power ratio low (PRL) of the captured signals. In [31] and [32], one of the three parameters used is established from the arithmetic mean of the spectral power for a frequency interval where the energy is more significant, thus identifying the frequency band that has spectral power components greater than 70%. Other widely used techniques, such as the chromatic technique [33], [34], [35] or the technique based on cumulative energy function and mathematical morphology gradient, are also based on characteristic parameters that are highly sensitive to spectral changes of PD signals [36], [37]. Another important information evidenced through the separation techniques, given the good sensitivity of some of the characteristic parameters used, is the possibility of quickly identifying changes in the visual representation of the clusters formed in the separation maps such as displacement of the points being grouped or changes in the shape and/or position of the clusters. This visual information is very useful when establishing whether the fault being monitored has evolved or an additional source of PD has appeared, since under both scenarios the dielectric properties of the insulation have changed and, consequently, the electrical parameters of the circuit have also changed, thus generating variations in the temporal and spectral behavior of the EM emissions and the pulses that propagate electrically [23]. For this reason, it is of great importance to know the effects that variations in the measurement environment can generate as a consequence of the inclusion or removal of obstacles in the UHF detection processes, since any physical change in the measurement environment could generate important changes in the information captured by the antennas and then these emissions could be erroneously associated with a new failure or an evolution of the fault being monitored, thus generating false alarms regarding the real situation of the asset. Additionally, many PD in UHF source identification systems are based on intelligent pattern recognition algorithms that are also trained and tested with characteristic parameters extracted from the spectral behavior of the pulses, or directly from the complete spectral information of the signals (for the entire frequency spectrum according to the bandwidth of the equipment) [38], [39], [40]. According to the characteristics of these algorithms, it is highly possible that when a spectral change is generated in the signals of the same PD source because of the removal or inclusion of obstacles in the measurement environment, the identification algorithm will classify them as signals from a completely different source (or noise) and consequently a wrong diagnosis process will be carried out.

III. Experimental Setup

To evaluate the behavior of the signals captured with a Vivaldi antenna in the presence or absence of obstacles in the measurement environment, two different experimental configurations were implemented using obstacles of different geometry (Fig. 2). The first setup consisted of eight rectangular obstacles of 10 × 10 and 150 cm high, equidistant to the PD source. The second experimental configuration was formed by cylindrical obstacles of 6.37 cm in diameter with a height of 150 cm. In both cases, the obstacles were located 40 cm away from the PD source in a circular array and the Vivaldi antenna was placed 16 cm between the PD source and the obstacles. Using rectangular obstacles allows for the assessment of how the edges and corners of square structures, such as components of electrical machines, distribution boxes, control panels, cabinets, enclosures, or switching equipment, influence the propagation of UHF signals emitted by PDs. Conversely, the inclusion of cylindrical obstacles enables replication of the effects observed with poles, transmission towers, conductors, or bus bars. The nonplanar geometry of these obstacles provides a more realistic representation of actual structures, facilitating a comprehensive evaluation of the signals' interaction with cylindrical shapes. It is important to acknowledge that while these selected obstacle shapes do not encompass the entire range of forms encountered in real environments, they were chosen for their ability to represent typical scenarios and simplify the assessment of their impact on the signals. In both configurations, two different test objects were used to generate stable PD activity for the measurement processes, and the obstacles were connected to the ground of the laboratory and the measurement circuit as well. The first test object was a methacrylate disk containing a cylindrical void 3 mm in diameter and 4 mm in height. This test object allows to obtain a stable internal PD activity at 13 kV. The second test object was a twisted pair of copper wires in which stable activity of surface PD was achieved at 10.3 kV.

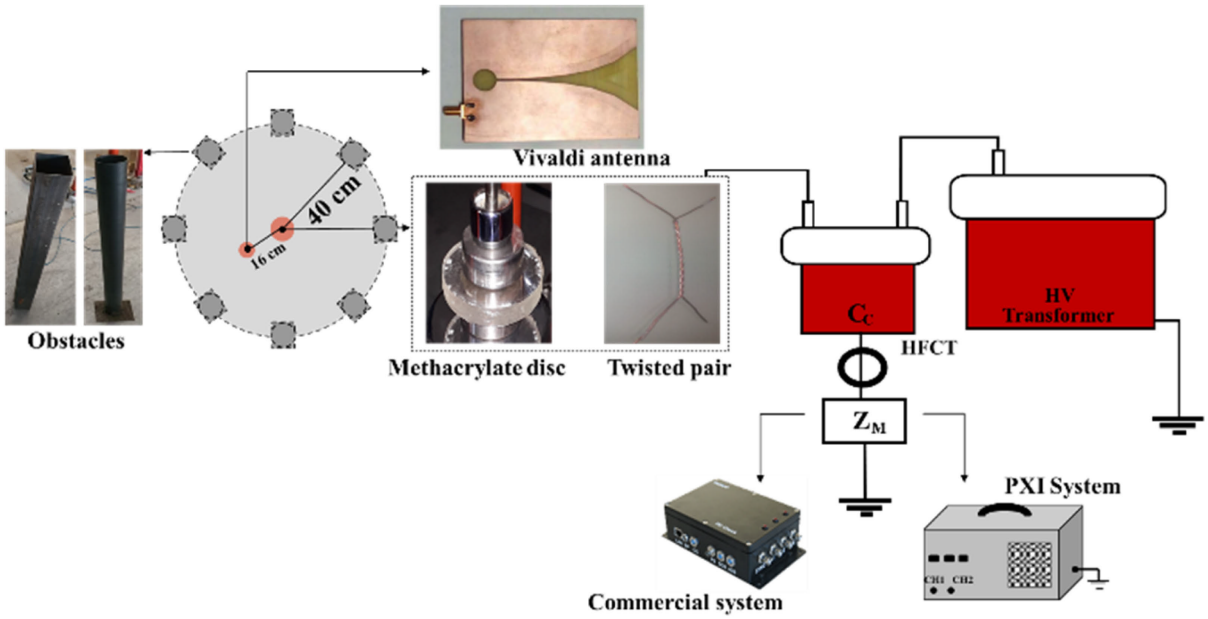

Fig. 2. Process of measurement, separation, and identification of PD sources.

TABLE I
VOLTAGE LEVELS FOR EACH MEASUREMENT PROCESS

Test object	No obstacles	With rectangular obstacles	With Cylindrical obstacles
Methacrylate disc	13 kV	13 kV	13 kV
Twisted pair	10.3 kV	10.3 kV	10.3 kV

From these two test objects, six different measurement processes were established, as described in Table I.

For each measurement, an indirect measurement circuit was used. As shown in Fig. 2, this circuit was formed by a PD-free high voltage source up to 100 kV, a 1 nF coupling capacitor (Cc), a measuring impedance or quadrupole (Zm), which delivered the sync signal and the PD pulses for a commercial PD monitoring system. The main objective of using this commercial system was to validate the presence of PD and the type of source captured (that is to recognize them as corona, surface, or internal PD). The acquisition system in charge of digitizing the signals captured by the Vivaldi antenna was programmed in LabVIEW and implemented on a PXI system that integrates an NI-PXIe-1082 chassis, an NIPXIe-8115 controller, and an NI-PXIe-5124 acquisition card with a sampling frequency of 6.25 Gs/s, 3 GHz of bandwidth, and 8-bit of vertical resolution. According to the programming, the system stored the PD pulses in time windows of 1 μs. The UHF sensor used for measuring EM emissions from PD was a Vivaldi antenna, which is commonly employed in UHF PD measurements [27]. The design of the Vivaldi antenna is specifically optimized for operating within the frequency range of 1.25–2.4 GHz. However, it also demonstrates efficient measurement capabilities for spectral power content below 1 GHz. Physically, this antenna is composed of an exponential slot line or waveguide embedded in a substrate, with a microstrip transmission line utilized to extract the signal to an SMA connector. Further details regarding this antenna and the measurement circuit employed can be found in [27] and [28]. Based on the optimized frequencies of the Vivaldi antenna, the PXI acquisition system was configured with a sampling rate of 4 GS/s.

IV. RESULTS AND DISCUSSION

For each test object, the measurement process begins by maintaining a low voltage level and a low trigger level in the acquisition system. In this way, the maximum amplitude of the background noise present in the measurement laboratory is established. The trigger level is then adjusted above the noise, and the voltage is increased until stable PD activity is obtained, thus guaranteeing the pulses captured by the Vivaldi antenna correspond to PD sources. Additionally, the commercial system allows the nature of the generated PD source to be always validated. The first measurement on each test object was performed without obstacles in the measurement environment, this group of signals was labeled as Ref1 (t) for the methacrylate disk and Ref2 (t) for the twisted pair. The second measurement process was performed keeping the test object and the antenna, adding rectangular obstacles around the test objects. The group of signals captured for the methacrylate disk on these conditions was labeled as SR-M (t), and the signals captured on the twisted pair were labeled as SR-TP (t). Finally, the third measurement process was carried out with cylindrical obstacles thus obtaining the group of signals associated with the methacrylate disk [SC-M (t)], and the twisted pair labeled as SC-TP (t). Consistent with the details provided in Section III, for the second and third measurement processes, the obstacles are positioned equidistantly around the test object and the antenna. Each group obtained during the different measurement processes was made up of around 200 signals captured in time windows of 1 μs. The normalized averaged

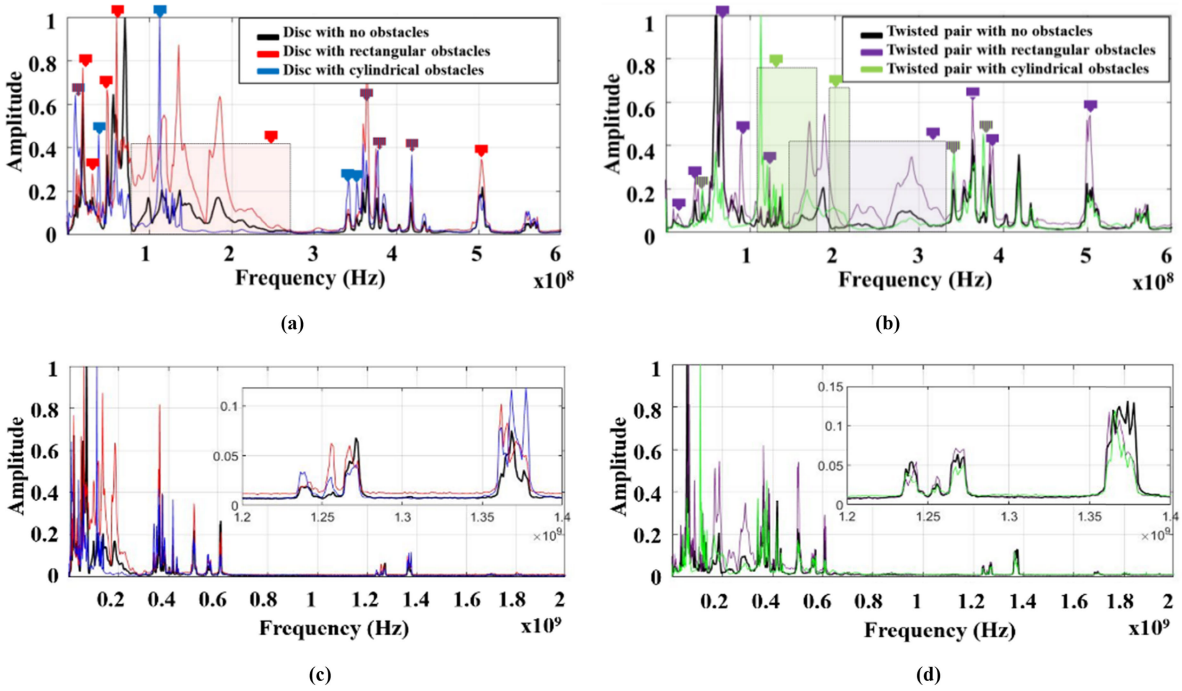

Fig. 3. Normalized mean spectral content of the UHF signals: (a) internal PD on methacrylate disk up to 600 MHz, (b) surface PD in twisted pair up to 600 MHz, (c) Internal PD on methacrylate disk up to 2 GHz, and (d) surface PD in twisted pair up to 2 GHz.

spectral power of the total signals was obtained to perform the analysis of the spectral behavior of the signals associated with each group. This allowed the identification, for each frequency band, of variations in the spectral content of each measurement group in the presence of the two types of obstacles.

A. Experimental Results With Rectangular Obstacles

Taking as reference the spectral content of the signals captured without obstacles Ref1 (t) and Ref2 (t) [black lines in Fig. 3(a) and (b)], it is observed that for the case of the methacrylate disk, when rectangular obstacles are in the measurement environment, the spectral content of SR-M (t) (red line) increases significantly in different intervals and frequency bands. Specifically, an increase in spectral power is observed over the interval [78–264] MHz and concretely in the frequency bands over 16, 22, 30, 45, 61, 361, 373, 419, and 504 MHz. Spectral power increases were also observed in Fig. 3(b) for the measurements made in the twisted pair keeping the same type of obstacles (purple line), where the increase in the spectral content of SR-TP (t) was significant for the interval [145–330] MHz and over the frequency bands around 16, 35, 42, 69, 92, 121, 340, 361, 373, 381, and 504 MHz. When evaluating the spectral contents of PD signals above 0.6 GHz in both test objects, no significant changes were observed in the spectral power of the captured signals, except for the increases in spectral power normally associated with amateurs and aeronautical radio navigation found around 1200- and 1350-MHz band, see Fig. 3(c) and (d). On the other hand, when including rectangular obstacles in the measurement environment, decreases in spectral power in certain intervals or frequency bands were evidenced with respect to the no obstacle reference case. To highlight this attenuation, the gain (G) for each group established in the measurement processes with obstacles was obtained up to 600 MHz according to the following:

$$G = 20 \cdot \log\left(\frac{\overline{S(f)}}{\overline{\mathrm{Ref}(f)}}\right) \tag{1}$$

where $\overline{S(f)}$ is the average fast Fourier transform (FFT) by frequency band for the group of signals where the measurement process was performed with obstacles, $\overline{\mathrm{Ref}(f)}$ is the average of the FFT per frequency band for the groups of signals obtained in measurements without obstacles [Ref1 (t) and Ref2 (t)]. As stated above, the analysis was carried up to 600 MHz, since the most significant changes in measurements with obstacles were observed in this frequency interval. According to Fig. 4(a) and (b), in the case of the group of measurements with rectangular obstacles on both test objects [SR-M(t) and SR-TP(t)], no significant attenuation was found by frequency intervals, except for some specific frequencies (52, 345, and 405 MHz in the methacrylate disk, and in the twisted pair at 57 and 412 MHz). According to the summarized results in Table II, the bands and frequency intervals where spectral power increases coincide for this type of obstacle are [145–264], 16, 92, 121, 361, 373, and 504 MHz. No coincidences were observed in the frequency bands where reductions in spectral power were observed for both test objects.

B. Experimental Results With Cylindrical Obstacles

According to Fig. 3(a), the group of signals SC-M associated with the source of internal PDs in the methacrylate disk (blue line), the spectral power increases are more specific and tend to occur in frequency bands around 16, 35, 111, 340, 349, 361, 373, and 419 MHz. On the other hand, in Fig. 3(b), it is observed that for the group of signals SC-TP (t) associated

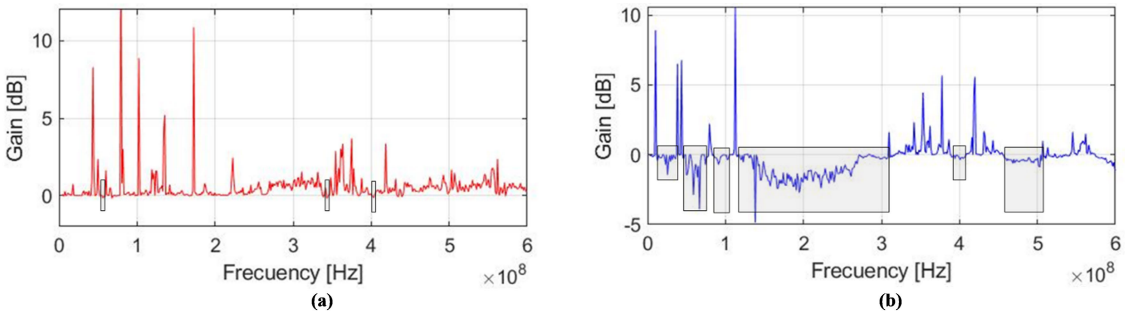

Fig. 4. Average gain by frequency bands for PD measurements with rectangular obstacles: (a) on methacrylate disks and (b) on twisted pair.

TABLE II
BANDS AND FREQUENCY INTERVALS WHERE CHANGES WERE OBSERVED DUE TO THE PRESENCE OF RECTANGULAR OBSTACLES

Group of signals	Frequencies with increased spectral power	Coinciding frequencies	Frequencies with decreased spectral power	Coinciding frequencies
SR-M(t)	[78-264] MHz, 16 MHz, 22 MHz, 30 MHz, 45 MHz, 61MHz, 361 MHz, 373 MHz, 419 MHz, and 504 MHz	[145-264], 16 MHz, 92 MHz, 121 MHz, 361 MHz, 373 MHz, and 504 MHz	52 MHz, 345 MHz, and 405 MHz	–
SR-TP(t)	[145-330] MHz, 16 MHz, 35 MHz, 42 MHz, 69 MHz, 92 MHz, 121 MHz, 340 MHz, 361 MHz, 373 MHz, 381 MHz, and 504 MHz		57 MHz and 412 MHz	

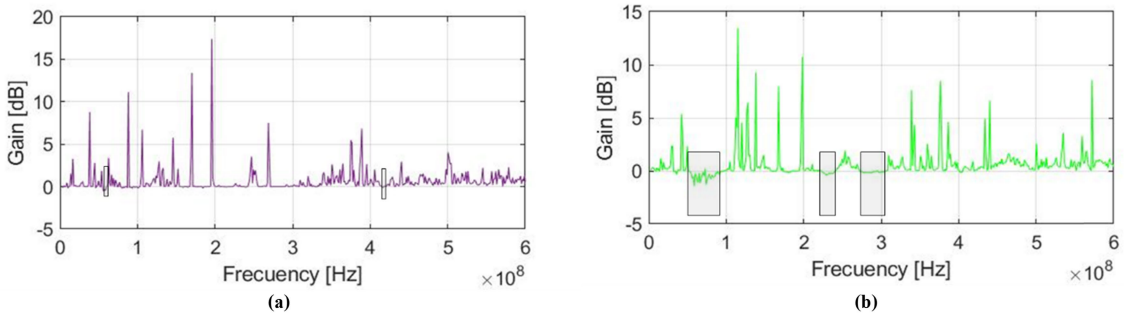

Fig. 5. Average gain by frequency bands for PD measurements with cylindrical obstacles: (a) in methacrylate disk and (b) in twisted pair.

with superficial PDs in the twisted pair (green line), the increases in spectral power are much greater, and are present in the intervals [106–176] MHz, [192–215] MHz, and in the bands of 42 340, and 373 MHz. When evaluating the spectral contents of PD signals above 1.2 GHz in both measurement processes, no significant changes in the spectral power content were observed.

In measurements with cylindrical obstacles on both test objects, the attenuation of spectral content is much larger than when rectangular obstacles were included. Fig. 5(a) shows that with cylindrical obstacles the spectral content of the measurements on the methacrylate disk [SC-M (t)] show significant decreases for the intervals [12–35], [47–70], [83–105], [114–312], [390–415], and [455–509] MHz.

In measurements with the twisted pair SC-TP (t) shown in Fig. 5(b), the attenuation of the spectral content is evident for the frequency bands [50–90], [225–240], and [273–306] MHz. Table III summarizes the bands and frequency intervals where spectral power increases and decreases were observed in both test objects due to the presence of cylindrical obstacles in the measurement environment. Unlike the previous case, the reduction in the spectral power in UHF PD signals is much more significant with this type of obstacles. It is noteworthy that both test objects share frequency intervals where this energy decrement is observed, specifically at [50–70], [83–90], [225–240], and [273–306] MHz.

V. INFLUENCE OF OBSTACLES IN THE SPECTRAL BEHAVIOR OF PD SIGNALS IN UHF

The previous results confirm that the spectral content of the PD signals in UHF is affected by the presence of obstacles in the measurement environment, generating increments, and decrements in the spectral power content for different bands or frequency intervals. Given that many of the source separation

TABLE III

BANDS AND FREQUENCY INTERVALS WHERE CHANGES WERE OBSERVED DUE TO THE PRESENCE OF CYLINDRICAL OBSTACLES

Group of signals	Frequencies with increased spectral power	Coinciding frequencies	Frequencies with decreased spectral power	Coinciding frequencies
SR-M(t)	16 MHz, 35 MHz, 111 MHz, 340 MHz, 349 MHz, 361 MHz, 373 MHz, and 419 MHz	111 MHz, 340 MHz, and 373 MHz	[12-35] MHz, [47-70] MHz, [83-105] MHz, [114-312] MHz, [390-415] MHz and [455-509] MHz	[50-70] MHz, [83-90] MHz, [225-240] MHz and [273-306] MHz
SR-TP(t)	[106-176] MHz, [192-215] MHz, 42 MHz, 340 MHz, and 373 MHz		[50-90] MHz, [225-240] MHz and [273-306] MHz	

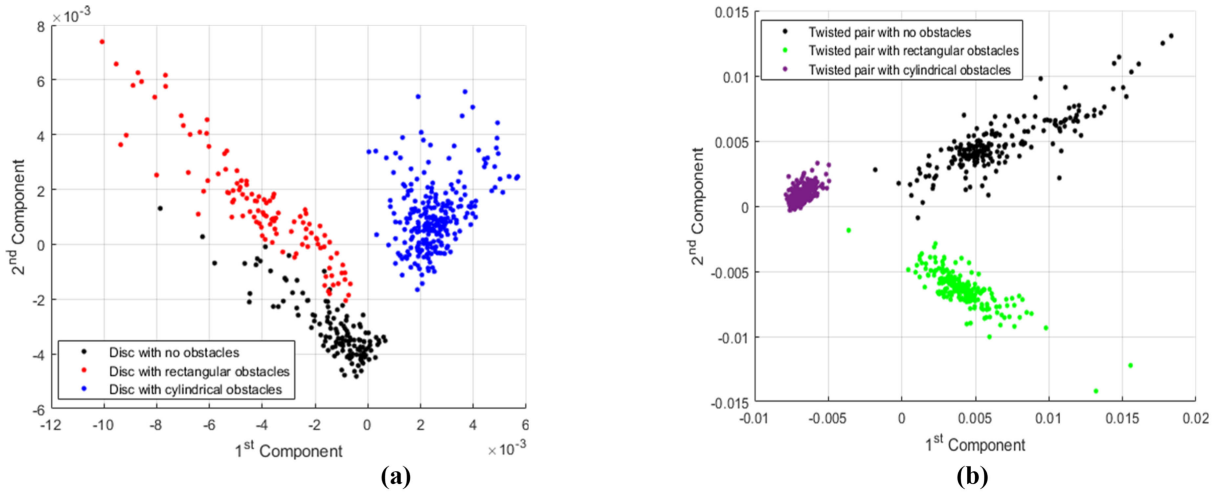

Fig. 6. Clusters found with PCA for measurements with and without obstacles in (a) methacrylate disk and (b) twisted pair.

and identification techniques use characteristic parameters extracted precisely from the spectral behavior of the signals, it is evident then that the variations produced in the spectral content of the UHF signals due to the presence of obstacles will generate alterations in the results delivered by these characteristic parameters. To demonstrate this effect more clearly in the clustering processes, where characteristic parameters based on the spectral behavior of the signals are used, the PCA was applied to the measurement sets obtained in both test objects for the three scenarios described in Section IV. One of the main advantages of using PCA to analyze each group is that it allows obtaining a graphical representation with the differences and similarities between datasets. For this analysis, the variable arrays were established for both test objects using the magnitude of the FFT of each signal as feature vector. As seen in Fig. 6, the differentiation between the clusters associated with each group is evident for both test objects. In the PCA plot of Fig. 6(a), with the measurements in the methacrylate disk, there is a short separation between the cluster associated with the signals with rectangular obstacles and the signals without obstacles. However, the cluster representing the group with cylindrical obstacles is completely separated from the other two clusters, confirming a clear differentiation in the frequency of the signals when obstacles are present in the measurement environment. In addition, it is confirmed that the influence of obstacles on the spectral content of the signals varies depending on the shape of the obstacles. In the case of measurements on the twisted pair, the separation of the clusters associated with each group is more evident since each cluster takes completely different positions on the separation map, see Fig. 6(b). Each group of signals previously characterized with PCA was represented on a map of separation to validate, in a real separation technique, that obstacles in the measurement environment can modify the characteristic parameters based on the spectral behavior of the signals. For this analysis, a 2-D separation map was established based on the characteristic parameters B (equivalent bandwidth) and Wc (average frequency or characteristic angular frequency) used in the chromatic separation technique, which has been widely used in different studies to separate PD sources into very high frequency (VHF) and UHF [15], [33], see equations as follows:

$$\omega_c = \frac{\int \omega \left| F(\omega))^2 d\omega \right|}{2\pi E_b} \tag{2}$$

$$B = \sqrt{\frac{1}{E_b} \int (\omega - \omega_c)^2 \left| F(\omega) \right|^2} \tag{3}$$

where $F(\omega)$ is the Fourier transform of the signal in time, ω is the angular frequency, and E_b is the signal energy content. Although with the chromatic technique it is possible to establish a 3-D separation map, in this case only the

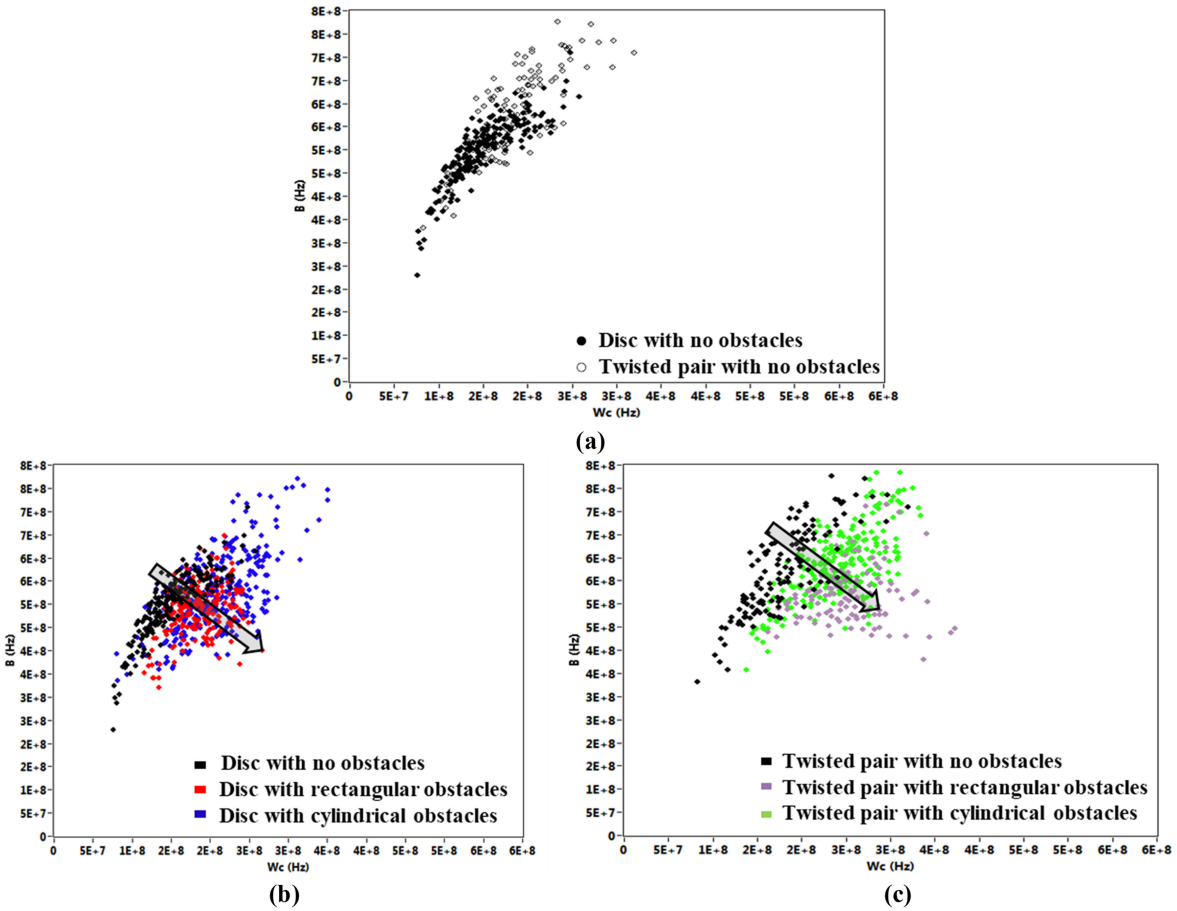

Fig. 7. Clusters found with the chromatic technique for the measurement groups in (a) disk and twisted pair with no obstacles: Ref1 (t) and Ref2 (t), (b) with and without obstacles in methacrylate disk, and (c) with and without obstacles in twisted pair.

two characteristic parameters that are directly related to the spectral behavior of the signals have been used. Fig. 7(a) represents the separation map with the clusters of the two reference measurements Ref1(t) and Ref2(t) obtained with both test objects without obstacles in the measurement. As can be seen, both clusters show a specific level of dispersion that will serve as a reference to identify changes in the clusters of the measurement processes that include obstacles. The separation maps in Fig. 7(b) and (c) show the groups of measurements made including the two types of obstacles. In each case, a displacement of the clusters and an increase in the dispersion of the points are observed, being more evident in the measurements with the twisted pair. As observed in both figures, the displacement of the clusters is produced by the increase in the dispersion in the data and tends to be carried out diagonally, toward the lower right part of the maps. These results, obtained with the chromatic separation technique, validate those observed with the analysis by frequency bands and the PCA graphs, clearly confirming the influence of obstacles in the results that deliver characteristic parameters of the UHF signals used to automatically separate or identify PD sources.

VI. Conclusion

The result presented in this work shows that the presence of obstacles in the measurement environment generates significant changes in the spectral content of the signals captured with the Vivaldi antenna. Although this UHF antenna is optimized for frequencies above 1 GHz, the results show that the frequency bands with the most evident spectral variations were below 600 MHz. According to the results, although there were no characteristic variation patterns that could be attributed to a specific type of obstacle, it was observed that the positive spectral gain was more frequent for measurements with rectangular obstacles, unlike cylindrical obstacles, in which the spectral gains were mostly negative. Finally, the application of PCA and the chromatic separation technique on the groups of signals obtained in the different measurement processes confirmed that the changes experienced by the signals because of the presence of obstacles in the measurement environment can significantly alter the results obtained with the characteristic parameters based on the spectral behavior of the PD signals, giving rise to important alterations in the shape and dispersion of the clusters.

References

[1] F. Kreuger, "*Partial Discharge Detection in High-Voltage Equipment*. London, U.K.: Butterworth, 1989.

[2] P. Gill, *Electrical Power Equipment Maintenance and Testing*. Boca Raton, FL, USA: CRC Press, 2008.

[3] E. Kuffel, W. Zaengi, and J. Kuffel, *High Voltage Engineering Fundamentals*. Oxford, U.K.: Butterworth-Heinemann, 2000.

[4] P. H. F. Morshuis, "Degradation of solid dielectrics due to internal partial discharge: Some thoughts on progress made and where to go now," *IEEE Trans. Dielectr. Electr. Insul.*, vol. 12, no. 5, pp. 905–913, Oct. 2005.

[5] Y. Shibuya, S. Matsumoto, M. Tanaka, H. Muto, and Y. Kaneda, "Electromagnetic waves from partial discharges and their detection using patch antenna," *IEEE Trans. Dielectr. Electr. Insul.*, vol. 17, no. 3, pp. 862–871, Jun. 2010.

[6] A. J. Reid, M. D. Judd, R. A. Fouracre, B. G. Stewart, and D. M. Hepburn, "Simultaneous measurement of partial discharges using IEC60270 and radio-frequency techniques," *IEEE Trans. Dielectr. Electr. Insul.*, vol. 18, no. 2, pp. 444–455, Apr. 2011.

[7] A. Contin, A. Cavallini, G. C. Montanari, G. Pasini, and F. Puletti, "Digital detection and fuzzy classification of partial discharge signals," *IEEE Trans. Dielectr. Electr. Insul.*, vol. 9, no. 3, pp. 335–348, Jun. 2002.

[8] R. Bartnikas and J. P. Novak, "On the character of different forms of partial discharge and their related terminologies," *IEEE Trans. Electr. Insul.*, vol. 28, no. 6, pp. 956–968, Dec. 1993.

[9] J. M. Martinez-Tarifa, J. A. Ardila-Rey, and G. Robles, "Automatic selection of frequency bands for the power ratios separation technique in partial discharge measurements—Part I, fundamentals and noise rejection in simple test objects," *IEEE Trans. Dielectr. Electr. Insul.*, vol. 22, no. 4, pp. 2284–2291, Aug. 2015.

[10] J. A. Ardila-Rey, J. M. Martinez-Tarifa, and G. Robles, "Automatic selection of frequency bands for the power ratios separation technique in partial discharge measurements—Part II, PD source recognition and applications," *IEEE Trans. Dielectr. Electr. Insul.*, vol. 22, no. 4, pp. 2293–2301, Aug. 2015.

[11] E. Montero, N. Medina, and J. Ardila-Rey, "An evaluation of meta-heuristic approaches for improve the separation of multiple partial discharge sources and electrical noise," in *Proc. IEEE 29th Int. Conf. Tools Artif. Intell. (ICTAI)*, Nov. 2017, pp. 1166–1173.

[12] J. A. Ardila-Rey, E. Montero, and N. M. Poblete, "Application of meta-heuristic approaches in the spectral power clustering technique (SPCT) to improve the separation of partial discharge and electrical noise sources," *IEEE Access*, vol. 7, pp. 110580–110593, 2019.

[13] F. Álvarez, F. Garnacho, A. Khamlichi, and J. Ortego, "Classification of partial discharge sources by the characterization of the pulses waveform," in *Proc. IEEE Int. Conf. Dielectrics (ICD)*, vol. 1, Jul. 2016, pp. 514–519.

[14] F. Alvarez, J. Ortego, F. Garnacho, and M. A. Sanchez-Uran, "A clustering technique for partial discharge and noise sources identification in power cables by means of waveform parameters," *IEEE Trans. Dielectr. Electr. Insul.*, vol. 23, no. 1, pp. 469–481, Feb. 2016.

[15] J. Zhang et al., "Chromatic classification of RF signals produced by electrical discharges in HV transformers," *IEE Proc.-Gener., Transmiss. Distrib.*, vol. 152, no. 5, pp. 629–634, Sep. 2005.

[16] J. A. Ardila-Rey, J. M. Martínez-Tarifa, M. Mejino, R. Albarracín, M. V. Rojas-Moreno, and G. Robles, "Chromatic classification of RF signals for partial discharges and noise characterization," in *Proc. IEEE Int. Conf. Solid Dielectrics (ICSD)*, Jun. 2013, pp. 67–70.

[17] J. Ardila-Rey et al., "A comparison of inductive sensors in the characterization of partial discharges and electrical noise using the chromatic technique," *Sensors*, vol. 18, no. 4, p. 1021, Mar. 2018.

[18] M.-X. Zhu et al., "Partial discharge signals separation using cumulative energy function and mathematical morphology gradient," *IEEE Trans. Dielectr. Electr. Insul.*, vol. 23, no. 1, pp. 482–493, Feb. 2016.

[19] M.-X. Zhu et al., "Self-adaptive separation of multiple partial discharge sources based on optimized feature extraction of cumulative energy function," *IEEE Trans. Dielectr. Electr. Insul.*, vol. 24, no. 1, pp. 246–258, Feb. 2017.

[20] V. Javandel, A. Akbari, M. Ardebili, and P. Werle, "Simulation of negative and positive corona discharges in air for investigation of electromagnetic waves propagation," *IEEE Trans. Plasma Sci.*, vol. 50, no. 9, pp. 3169–3177, Sep. 2022.

[21] K. C. Ghanakota, Y. R. Yadam, S. Ramanujan, P. V. J. Vishnu, and K. Arunachalam, "Study of ultra high frequency measurement techniques for online monitoring of partial discharges in high voltage systems," *IEEE Sensors J.*, vol. 22, no. 12, pp. 11698–11709, Jun. 2022.

[22] C. Boya, M. V. Rojas-Moreno, M. Ruiz-Llata, and G. Robles, "Location of partial discharges sources by means of blind source separation of UHF signals," *IEEE Trans. Dielectr. Electr. Insul.*, vol. 22, no. 4, pp. 2302–2310, Aug. 2015.

[23] C. Madariaga, R. Schurch, J. Ardila-Rey, O. Muñoz, and S. Fingerhuth, "Partial discharge electrical tree growth identification by means of waveform source separation techniques," *IEEE Access*, vol. 9, pp. 64665–64675, 2021.

[24] S. Coenen, S. Tenbohlen, S. M. Markalous, and T. Strehl, "Sensitivity of UHF PD measurements in power transformers," *IEEE Trans. Dielectr. Electr. Insul.*, vol. 15, no. 6, pp. 1553–1558, Dec. 2008.

[25] R. Albarracín, J. Ardila-Rey, and A. Mas'ud, "On the use of monopole antennas for determining the effect of the enclosure of a power transformer tank in partial discharges electromagnetic propagation," *Sensors*, vol. 16, no. 2, p. 148, Jan. 2016.

[26] *High-Voltage Test Techniques: Partial Discharge Measurements*, Standard IEC-60270, 2000, pp. 13–31.

[27] G. Robles, R. Albarracín, J. L. Vázquez, and Z. Chen, "Antennas in partial discharge sensing system," in *Handbook of Antenna Technologies*, vol. 3. Singapore: National Univ. of Singapore, Department of Electrical and Computer Engineering, 2015, pp. 2419–2474. [Online]. Available: https://link.springer.com/referenceworkentry/10.1007/978-981-4560-44-3_95

[28] R. Albarracin, G. Robles, J. M. Martinez-Tarifa, and J. Ardila-Rey, "Separation of sources in radiofrequency measurements of partial discharges using time-power ratio maps," *ISA Trans.*, vol. 58, pp. 389–397, Sep. 2015.

[29] Z. Li et al., "A pulse interference suppression method based on double-sensor detection for PD measurement in frequency-tuned resonant tests," *IEEE Trans. Instrum. Meas.*, vol. 71, pp. 1–8, 2022.

[30] M. D. Judd, L. Yang, and I. B. B. Hunter, "Partial discharge monitoring for power transformer using UHF sensors. Part 2: Field experience," *IEEE Elect. Insul. Mag.*, vol. 21, no. 3, pp. 5–13, May/Jun. 2005.

[31] S. Ning, Y. He, L. Yuan, Y. Sui, Y. Huang, and T. Cheng, "A novel localization method of partial discharge sources in substations based on UHF antenna and TSVD regularization," *IEEE Sensors J.*, vol. 21, no. 15, pp. 17040–17052, Aug. 2021.

[32] G. V. R. Xavier, H. S. Silva, E. G. da Costa, A. J. R. Serres, N. B. Carvalho, and A. S. R. Oliveira, "Detection, classification and location of sources of partial discharges using the radiometric method: Trends, challenges and open issues," *IEEE Access*, vol. 9, pp. 110787–110810, 2021.

[33] J. A. Ardila-Rey, R. Schurch, N. M. Poblete, S. Govindarajan, O. Muñoz, and B. A. de Castro, "Separation of partial discharges sources and noise based on the temporal and spectral response of the signals," *IEEE Trans. Instrum. Meas.*, vol. 70, pp. 1–13, 2021.

[34] L. Wang, A. Cavallini, G. C. Montanari, and L. Testa, "Evolution of PD patterns in polyethylene insulation cavities under AC voltage," *IEEE Trans. Dielectr. Electr. Insul.*, vol. 19, no. 2, pp. 533–542, Apr. 2012.

[35] A. Cavallini, G. C. Montanari, A. Contin, and F. Pulletti, "A new approach to the diagnosis of solid insulation systems based on PD signal inference," *IEEE Elect. Insul. Mag.*, vol. 19, no. 2, pp. 23–30, Mar. 2003.

[36] J. A. Ardila-Rey, M. Cerda-Luna, R. Rozas-Valderrama, B. A. de Castro, A. L. Andreoli, and B. Cevallos, "A new technique for separation of partial discharge sources and electromagnetic noise in radiofrequency measurements using energy ratios of different antennas," *High Voltage*, vol. 6, no. 3, pp. 525–530, Jun. 2021.

[37] H. Janani and B. Kordi, "Towards automated statistical partial discharge source classification using pattern recognition techniques," *High Voltage*, vol. 3, no. 3, pp. 162–169, Sep. 2018.

[38] G. Robles, E. Parrado-Hernández, J. Ardila-Rey, and J. M. Martínez-Tarifa, "Multiple partial discharge source discrimination with multiclass support vector machines," *Exp. Syst. Appl.*, vol. 55, pp. 417–428, Aug. 2016.

[39] O. H. Abu-Rub, Q. Khan, S. S. Refaat, and H. Nounou, "Cable insulation fault identification using partial discharge patterns analysis," *IEEE Can. J. Electr. Comput. Eng.*, vol. 45, no. 1, pp. 31–41, Winter. 2022.

[40] J. Yeo et al., "Identification of partial discharge through cable-specific adaption and neural network ensemble," *IEEE Trans. Power Del.*, vol. 37, no. 3, pp. 1598–1607, Jun. 2022.

Jorge Alfredo Ardila-Rey (Member, IEEE) received the B.Sc. degree in mechatronic engineering from Universidad de Pamplona, Pamplona, Colombia, in 2007, the Specialist Officer degree in naval engineering from Escuela Naval Almirante Padilla, Cartagena, Colombia, in 2008, and the M.Sc. and Ph.D. degrees in electrical engineering from Universidad Carlos III de Madrid (UC3M), Madrid, Spain, in 2012 and 2014, respectively.

He was an Automatic Control Engineer of ARC Almirante Padilla, Cartagena, Colombia, from 2008 to 2010. From 2010 to 2014, he worked with the Department of Electrical Engineering and the High-Voltage Research and Test Laboratory (LINEALT), UC3M. He is currently working as a Professor with the Department of Electrical Engineering, Universidad Técnica Federico Santa María, Santiago, Chile. His research interests include data clustering, Structural Health Monitoring (SHM) systems, partial discharges, insulation systems diagnosis, and instrumentation and measurement techniques for high frequency currents.

Bruno Albuquerque de Castro (Senior Member, IEEE) received the B.Sc., M.Sc., and Ph.D. degrees in electrical engineering from São Paulo State University, Sao Paulo, Brazil, in 2012, 2016, and 2019, respectively.

The doctorate was achieved with a period at the Aerospace Centre, University of Surrey, Guildford, U.K. He is an Assistant Professor at the Electrical Engineering Department, São Paulo State University. His research field focuses on nondestructive inspection, electronic instrumentation, sensors, digital signal processing, acoustic emission, data acquisition, and intelligent systems.

Dr. de Castro is an Associate Editor of IEEE TRANSACTIONS ON INSTRUMENTATION AND MEASUREMENT (TIM).

Rodrigo Rozas-Valderrama was born in Punta Arenas, Chile, in 1984. He received the B.Sc. degree in electrical engineering and the master's degree in energy economics from the Universidad Técnica Federico Santa María, Santiago, Chile, in 2010 and 2016, respectively.

From 2010 to 2018, he worked as a Specialist Engineer in power system for Colbún S.A., Santiago de Chile, Chile, the second biggest power generation company. He is currently a Professor at the Department of Electrical Engineering, Universidad Técnica Federico Santa María. His research interests include partial discharges, insulation systems diagnosis, power system stability, power plants and instrumentation, and measurement techniques.

Luis Orellana was born in San Fernando, Chile, in 1992. He received the B.S. and M.S. degrees in electrical engineering from Federico Santa María Technical University, Santiago, Chile, in 2015 and 2019, respectively.

He has experience in studying the relationship between the electromagnetic burst and other diagnostics from dense plasma focus devices at the Plasma and Nuclear Fusion Laboratory, Chilean Nuclear Energy Commission. His research interests include high-power pulse technology, applied plasma physics, and signal analysis.

Carlos Boya received the degree in electrical and electronic engineer from the Technological University of Panama, Panama City, Panama, in 2001, and the master's and Ph.D. degrees in electrical, electronic and automatic engineering from the Carlos III University of Madrid, Madrid, Spain, in 2012 and 2018, respectively.

He is the director of the School of Industrial Technology of the Higher Specialized Technical Institute (ITSE) in Panama City, Panama and associate researcher at the Inter-American University of Panama and Leader of the High Voltage Electrical Testing Laboratory (LEEAT) at this university. He has more than 10 years of experience as a designer, inspector and project manager for electrical companies focused on the construction and management of high voltage lines. His research work focuses on the application of signal processing techniques and machine learning to different areas of engineering, such as: power electrical systems, electrical market, biomedical, acoustics, in addition to working in a line of research focused on educational robotics.

Firdaus Muhammad-Sukki received the M.Eng. degree in electrical and electronic engineering from the Imperial College, London, U.K., in 2006, and the postgraduate and Ph.D. degrees from Glasgow Caledonian University, Glasgow, U.K., in 2009 and 2013, respectively.

He is a Chartered Engineer, a member of the Institution of Engineering and Technology (IET), and an Associate of the City and Guilds, London (ACGI), U.K. He is a lecturer at the School of Engineering and Built Environment, Edinburgh Napier University. He has secured multiple grants from the UK and international funding agencies such as Innovate UK, Scottish Institute for Remanufacturing (SIR), Scottish Funding Council, British Council - Newton Fund, Chilean Research Council (CONICYT), Ministry of Higher Education Malaysia, Universiti Teknologi Malaysia etc. He also carried out a number of non-technical research including market trend and financial analysis related to renewable technologies for various countries. He has published numerous articles in high impact factor journals (e.g. Nature, Renewable and Sustainable Energy Reviews, Applied Energy, etc.), as well as presenting in various conferences related to his area. Prior to joining the academia, he was a communication engineer in Malaysia's largest telecommunication company. His research interest is in the area of renewable energy technology and policies and sustainable resources.

Abdullahi Abubakar Mas'ud received the B.Eng. and M.Sc. degrees in electrical engineering from Ahmadu Bello University, Zaria, Nigeria, in 1999 and 2006, respectively, and the Ph.D. degree in high voltage engineering from Glasgow Caledonian University, Glasgow, U.K., in 2013, under the supervision of Prof. Brian Stewart and Prof. Scott McMeekin. He completed his thesis on the application of ensemble neural network for partial discharge pattern recognition.

In 2002, he became an Assistant Lecturer at the Faculty of Engineering, Ahmadu Bello University. He is currently an Associate Professor at the Department of Electrical and Electronic Engineering, Jubail Industrial College, Jubail, Saudi Arabia. He has published a number of articles in high impact factor journals (e.g., *Renewable and Sustainable Energy Reviews*, *Renewable Energy*, *Energies*, *Sensors*, and so on) and presented papers in various conferences in the area of high voltage partial discharge and renewable energy.

Dr. Mas'ud is a member of the IET, International Association of Engineers, and a registered Engineer (COREN) Nigeria.